Submitted to ADVANCED MATERIALS

DOI: 10.1002/adma.201103591

Direct and Seamless Coupling of TiO_2 Nanotube Photonic Crystal to Dye-Sensitized Solar Cell: A Single-Step Approach

By *Cho Tung Yip,[+] Haitao Huang,[+,] * Limin Zhou,* Keyu Xie, Yu Wang, Tianhua Feng, Jensen Li, and Wing Yim Tam*

Dr. C. T. Yip, Prof. L. Zhou
Department of Mechanical Engineering
The Hong Kong Polytechnic University
Hung Hom, Kowloon, Hong Kong
E-mail: mmlmzhou@inet.polyu.edu.hk

Prof. H. Huang, K. Xie, Prof. Y. Wang
Department of Applied Physics and Materials Research Center
The Hong Kong Polytechnic University
Hung Hom, Kowloon, Hong Kong,
E-mail: aphhuang@polyu.edu.hk

T. Feng, Prof. J. Li,
Department of Physics and Materials Science
City University of Hong Kong
Tat Chee Avenue, Kowloon, Hong Kong

Prof. W. Y. Tam
Department of Physics
Hong Kong University of Science and Technology
Clear Water Bay, Kowloon, Hong Kong

[+] C. T. Y. and H. H. contributed equally to this work.

Keywords: photonic crystal, dye-sensitized solar cell, TiO_2 nanotubes, electrochemical anodization

Among various types of photovoltaic devices,[1-4] dye sensitized solar cells (DSSCs) are recognized as the viable one to compete with others, being inexpensive and able to be mass produced using simple fabrication processes.[3] Apart from the many chemical methods to enhance the efficiency of DSSCs, such as the purification of dye molecules[5] and surface treatment with $TiCl_4$,[6] physical methods are also frequently used. A typical example is the use of a photonic crystal (PC) layer on top of the mesoporous TiO_2 layer to enhance light harvesting within the specific absorption spectrum range of the dye.[7-14] A variety of mechanisms are responsible for the enhancement of photovoltaic performance by coupling a

PC layer to the solar cell absorption layer, such as, 1) photon localization and enhanced red light absorption near the edges of a photonic bandgap,[8,15] 2) light reflection within the photonic bandgap at various angles,[16,17] and 3) formation of photon resonance modes within the dye-sensitized layer.[18,19] By tuning the thicknesses of the light absorbing TiO_2 and PC layers so as to control the reflected, diffracted, or refracted light passing through the cell,[17,20] a more significant improvement in light absorption can be achieved than the one caused by using geometrical optics based elements, such as the incoherent scattering layers and high-reflectivity metallic mirrors.[18,20]

Experimentally, there are many ways to couple the PC to the mesoporous TiO_2 layer in DSSC. In traditional PC-coupled DSSCs, the PC and absorbing TiO_2 layers are prepared by different processing methods and sometimes different materials, such as, depositing alternate layers of SiO_2 and TiO_2[11,19] or forming TiO_2 inverse opal layer[7,13,21] on top of the absorbing TiO_2 layer. However, these methods suffer from one or more of the following intrinsic drawbacks: (1) poor physical contact between the PC layer and the TiO_2 absorbing layer; (2) non-conductive PC layer that hinders the charge transport (leading to poor fill factor); (3) clogging channels (for electrolyte infiltration) formed at the interface; (4) the photonic bandgap being impossible to be continuously adjusted for the maximization of light harvesting; and (5) stringent requirement on interface flatness laid by the processing method, restricting the thickness of the absorbing layer to be very thin. Although PC-coupled DSSCs are reported to be better than those without PC coupling, a poor fact is that all the existing PC-coupled DSSCs suffer from relatively low power conversion efficiencies due to the above intrinsic drawbacks.

In the present study we have developed a novel approach to overcoming all the above drawbacks. Both the absorbing TiO_2 and PC layers were fabricated by electrochemical anodization, where the PC layer was fabricated by anodization under periodic current pulses. The schematic of the bi-layer structure fabrication and cell assembly processes is shown in

Figure 1. Apart from overcoming the above mentioned drawbacks, an added value of this coupling technique is that the PC layer also contributes to the light conversion by its response to localized photons near the long wavelength edge of the photonic bandgap. Moreover, the TiO_2 absorbing layer formed by anodization is actually one-dimensional nanotube (NT) array whose electron-hole recombination is reported to be much slower than that of mesoporous TiO_2 nanoparticles, while the electron transport time is similar in both nanostructures.[22] Remarkable increase in power conversion efficiency has been achieved in DSSC adopting this novel bi-layer structure.

The key to obtaining a perfect PC layer is the formation of an ideal periodic structure along the axial direction of the NTs. Anodization under periodic voltage pulses fails to form PC since the structural period decreases with time.[23] Close examination of the anodization process shows that the formation of TiO_2 NT involves competition between the oxidation of metallic Ti at the bottom of the NTs and the dissolution of TiO_2.[24] If the dissolution of TiO_2 at the mouth of NTs can be kept to a minimum by using an organic based electrolyte such as ethylene glycol,[25,26] the growth rate of TiO_2 NTs is then controlled by the oxidation of Ti to TiO_2 under stable conditions. The growth rate of TiO_2 NTs is hence dependent on the rate of charge transferred to the external circuit, i.e., the current. Therefore, to obtain a periodic structure along the axial direction of NTs, a periodic current anodization method should be used. A similar method using constant current pulses to obtain a periodic structure has been reported.[27]

Figure 2 shows a dense array of smooth-walled NTs with a periodic structure along the axial direction obtained by anodization using periodic constant current pulses. The voltage-time transient for a particular anodization process is also shown. The as-anodized PC layer showed a purple color under fluorescent light. When it was transferred to the fluorine doped tin oxide (FTO) glass substrate and immersed in ethanol, a nearly green color was observed. This red shift of the spectral reflection peak is due to the lowering of the refractive index

contrast of the PC layer. This result agrees quite well with the theoretical calculations (**Figure S5**, Supporting Information). The reflection peak of the PC layer can be easily tuned by adjusting the axial lattice constant through monitoring the current pulse durations (t_{HC} and t_{LC}).

Optical properties. As-anodized TiO_2 PC layers with different periods (but fixed lattice constant around 150 nm) were detached from the Ti substrates and attached to FTO substrates for reflectance measurements. As can be seen from **Figure 3**a, under near normal incidence of unpolarized light, a broad peak centered at around 430 nm (purple sample in air) was observed, with maximum reflectance of around 60% and additional features at longer wavelengths. The reflectance spectra were strongly affected by the refractive index contrast. For example, when the sample was infiltrated with ethanol, a red shift of the reflection peak could be observed, compared with that of the sample in air. When the refractive index contrast was further lowered by infiltration with the liquid electrolyte (the hole-transporting medium of DSSCs), the reflection peak of the PC layer shifted to an even longer wavelength which was close to one of the absorption peaks (~500 nm) of the N719 dye. Numerical simulations were conducted on the TiO_2 PC layer and the simulated reflectance spectra agreed well with the experimental results in terms of peak position (Figure 3 and Figure S5, Supporting Information). The secondary oscillating feature in simulated spectra was not experimentally observed due to microstructure imperfections. Moreover, the intensity of Bragg reflection increased with increasing number of periods in the PC layer (Figure 3). Similar results were obtained for the PC layer with an axial lattice constant of 180 nm (green sample in air, Figure 3b). The reflection peak of this sample in electrolyte was located at near infrared (~640 nm), which is in the low absorption region of N719. Furthermore, by tuning the HC duration during anodization, a variety of differently colored PC layers could be fabricated (Figure 2c). This feature allows us to match at will the bandgap of the PC layer (in electrolyte) to any appropriate absorption region of any dye molecules for DSSC applications. The continuously adjustable bandgap of the anodic PC layer is an attractive feature for maximizing the

photovoltaic performance of DSSCs. While in conventional methods, such as the inverse opal template one, only discrete bandgap can be obtained due to the discrete size of polystyrene spheres.

Photovoltaic characteristics. To demonstrate the effect of PC layer on the photovoltaic performance of DSSCs, cells with the bi-layer structure were compared with the reference cells without a PC layer. A total of 4~6 cells were tested for each type of cell. The thickness of the bi-layer structure in all the cells was around 10μm (Figure S2, Supporting Information), same as the thickness of the absorbing TiO_2 NT layer in a reference cell (Figure S3, Supporting information). As the dye adsorption varied in different samples, only those DSSCs with similar dye loading were chosen for comparison.

Figure 4 shows that all the DSSCs with a PC layer have better photovoltaic performance than the reference. Due to the presence of the PC, both the short circuit current J_{sc} and the open circuit voltage V_{oc} were improved. The increase in J_{sc} was due to the efficient light harvesting facilitated by the PC layer. It is expected that the increased photoelectron density, which is proportional to the product of J_{sc} and the recombination time constant,[22] will give rise to an increased V_{oc}.

To study the significance of the PC layer in light harvesting, the external quantum efficiency (EQE) was measured and the results are shown in **Figure 5**. It can be seen that under back side illumination, the PC effect leads to a significant lowering of EQE in the photonic bandgap region since the PC layer blocks the transmission of photons of this range to the NT absorbing layer. Under front side illumination, the use of PC layer leads to an increase of EQE within the photonic bandgap, corresponding to the maximum reflectance range of the PC layer. If the photonic bandgap is tuned towards a longer wavelength, the shape of EQE spectra will also change accordingly with the increase of EQE shifted to a longer wavelength. Due to the effective reflection of waves in the photonic bandgap and possible formation of resonance modes in the TiO_2 NT absorption layer, an enhanced

photocurrent response can thus be expected in DSSCs coupled by the PC layer. It should be noted that, if the PC layer was prepared by a conventional inverse opal method, a thin overlayer with a thickness around 100 nm is inevitably deposited, which will affect the resonance mode.[28,29] The ovelayer will introduce modifications in the photonic bandgap and also modulate the reflected light intensity in the pass band.[28] The technique used in the current work did not introduce any overlayer on top of the PC layer, as can be verfied from the cross-section SEM image (Figure S1, supporting information). This is another advantage of our technique. In our PC-coupled DSSC, an absorbing TiO_2 NT layer (without periodicity in the axial direction) has a total length of 5.5 μm on top of the PC layer. Resonance peaks are expected to appear in the reflection spectra, as explained by Mihi *et al*.[28] The peaks should repeat themselves at roughly regular intervals in wavelength while the width of this repetition depends on the thickness of the overlayer. When the thickness is gradually increased from zero, there will be a dip first appearing at the reflection peak.[28] When the thickness of the overlayer is further increased, more features (peaks and troughs) appear. For our case, we can estimate that the small featured peaks should repeat at around every 9 nm in wavelength and therefore they are averaged out already due to a little bit randomness in periodicity during the fabrication. More over, at energies below the photonic bandgap (Figure S7, Supporting Information), the standing wave is predominately localized at the high refractive index part of the PC structure[8] where the dye molecules are attached, photocurrent at longer wavelengths (than the photonic bandgap edge) will be increased. This is unambiguously illustrated in the EQE curve under back side illumination (Figure 5a) where a sharp peak around 600 nm can be seen.

Our results show that by coupling the PC layer to the TiO_2 NT absorbing layer an increase of over 50% in power conversion efficiency can be achieved in comparison with the efficiency of a DSSC without a PC layer. Such remarkable increase (50%) is rarely reported in PC-coupled DSSCs and moreover, the efficiency of our DSSC (5.61%) is higher than that

of most of the reported PC-coupled DSSCs.[7,9,11,14,30,31] It should be emphasized that the increase in conversion efficiency in our DSSC is not attributable to higher dye loading, and we only compared DSSCs with similar amounts of dye loading in Figure 4 in an attempt to study the effect of PC layer coupling. We believe that by optimizing the geometry of the electrode, tuning the photonic bandgap or using double PC layers,[32] increasing the dye loading, treating with $TiCl_4$, and using purer dye, the power conversion efficiency of our PC coupled DSSCs can achieve a value that appeal to the industry. To verify this belief, a prelimenary study was conducted. By varying the thickness of each layer and the axial period of the PC layer, a power conversion efficiency of 7.11% can be achieved (Figure S8, Supporting Information).

In summary, we have developed a single-step approach to the seamless coupling of a PC layer to a TiO_2 NT absorbing layer for greatly enhanced photovoltaic performance of DSSC. The TiO_2 NT layer was fabricated by normal electrochemical anodization and the TiO_2 PC layer was obtained by a periodic current pulse anodization. DSSCs equipped with this bi-layer structure showed significantly enhanced power conversion efficiency, an increase of over 50% compared with the cells without a PC layer (under simlar total thickness and dye loading). This improvement is attributed to the enhanced light harvesting of the DSSCs in the spectral range corresponding to the photonic bandgap of the PC and a longer wavelength range. The current technique of coupling the PC layer to the TiO_2 absorbing layer is superior to many others that use either inverse opals or periodic double layers, in that it provides a continuously tunable optical bandgap and leaves plenty of rooms for further enhancement in power conversion efficiency. Besides, this simple photonic crystal fabrication process can be extend to other applications, such as, DSSCs with solid state or viscous electrolyte, and plasmonic PC by metal infiltration into PC nanotubes, etc.

Experimental

*Fabrication of Bi-layer Structure***:** Titanium foils with a thickness of 0.25 mm were cleaned by sonication in ethanol for five minutes, then rinsed by deionized water (DI) and finally dried in an oven at 100 °C for 10 minutes. The electrolyte used for the anodization was ethylene glycol (99.8%, GR Ph Eur international laboratory) with 0.5 wt% ammonium fluoride (99+%, BDH) and 4-6 vol% DI water. Periodic current pulse anodization with high current (HC, J_{HC}=~8 mA cm^{-2}) and low current (LC, J_{LC}=0) was first adopted to fabricate the TiO_2 PC layer on the titanium foil. The value of the HC current was so determined to achieve a voltage of around 60 V between the titanium anode and the platinum counter electrode with a separation of 2.5 cm. The number of pulses and the pulse duration determined the number of periods and the length of period in the PC layer, respectively, and hence the optical properties. The as-anodized sample was heat-treated at 290°C for 3h followed by a single constant current anodization (~8 mA cm^{-2}) process to form a smooth-walled TiO_2 NT layer beneath the PC layer. The as-grown bi-layer structure was further heat treated at 290°C for 3h. A highly periodic PC layer can be seen to seamlessly grown on the NT layer (Figure S1, Supporting Information), ensuring good connection between the two layers and easy electrolyte infiltration.

Fabrication of DSSC: (1) The bi-layer membrane was detached from the Ti substrate and then adhered to the FTO substrate with TiO_2 nanoparticles (particle size around 13 nm and total thickness around 2 μm) using a sol-gel method. (2) The adhered samples were annealed at 450°C for 3h under heating and cooling rates of 1°C min^{-1}. (3) The samples were then soaked in a dye-containing solvent (0.3 mM N719 in ethanol) at room temperature for 18h, followed by rinsing in pure ethanol for 1 minute to remove non-chemisorbed dye, before being assembled in solar cells, i.e., sandwiched between two electrodes (FTO electrode and Pt-coated glass counter electrode) with a spacer layer (25 μm thickness, SX1170–25, Solaronix) and melted at 90°C to fix the separation. The electrolyte (DMPD:1.0M, LiI: 0.1M, 4-TBP:0.5M, I_2:0.12M, 3-methoxy propionitrile (MePN)) was infiltrated into the cells by placing

the electrolyte droplet in the cavity of the active area of the device before the device was sealed with UV epoxy.

Characterizations: Reflectance spectra were acquired using a typical microreflectivity/ microtransmission system (Ocean Optics(R) USB2000 + fiber spectrometer) over a sample area of roughly 5×5 μm^2 with magnification 100×. A spectral range of 400–900 nm was explored using a tungsten–halogen lamp. A field emission scanning electron microscope (JEOL JSM-6340F and LEO1530) was used to study the microstructure. I-V characteristics were measured by a Keithley 2420 source meter. For white-light efficiency measurements (at 100 mW cm^{-2}), a Newport 91160 solar-light simulator with an AM 1.5 filter was used. All the measurements were performed in air over an active area of 0.16 cm^2. For EQE measurement, the light source was from a Newport 66902 solar simulator. The wavelength of light was tuned with a Newport 74125 monochromator. The photocurrent was measured with a Newport 2931-C power meter. The light intensity was measured with a Newport 2931-C power meter equipped with a 71675_71580 detector probe.

Simulation: Finite-element full wave simulation (COMSOL Multiphysics) was employed for numerical calculation of reflection spectra. The photonic crystals were modeled as TiO_2 nanotubes arranged in a hexagonal lattice in the plane of titanium foil, with the axial geometric dimensions obtained from SEM graphs of the actual samples.

Dye Desorption Measurement: The dye (N719) adsorbed on the TiO_2 electrode was detached in 0.1M NaOH water solution for several days, and the absorption intensity of the dye solution was measured by UV-Vis spectrophotometer (UV-2550).

Supporting Information

Supporting Information is available from the Wiley Online Library or from the author.

Acknowledgement. The authors are grateful for the grants received from the Research Grants Council of the Hong Kong Special Administrative Region (PolyU 5349/10E and PolyU 5187/09E) and Hong Kong Polytechnic University (A-PJ46). The authors thank Jenny Hung for assistance in reflectance measurement, Ren Xiaochen for taking photos, and W.K.Sin for drawing the schematic diagram.

Received: ((will be filled in by the editorial staff))
Revised: ((will be filled in by the editorial staff))
Published online: ((will be filled in by the editorial staff))

[1] S. E. Shaheen, D. S. Ginley, G. E. Jabbour, *MRS Bull*. **2005**, *30*, 10 and references therein.

[2] A. Slaoui, R. T. Collins, *MRS Bull*. **2007**, *32*, 211 and references therein.

[3] B. O'Regan, M. Gratzel, *Nature*. **1991**, *353*, 737.

[4] H. Huang, *Nature Photon.* **2011**, *4*, 134.

[5] M. K. Nazeeruddin, F. De Angelis, S. Fantacci, A. Selloni, G. Viscardi, P. Liska, S. Ito, T. Bessho, M. Gratzel, *J. Am. Chem. Soc.* **2005**, *127*, 16835.

[6] B. O' Regan, J. R. Durrant, P. M. Sommeling, N. J. Bakker, *J. Phys. Chem. C*. **2007**, *111*, 14001.

[7] S. Guldin, S. Huttner, M. Kolle, M. E. Welland, P. Muller-Buschbaum, R. H. Friend, U. Steiner, N. Tetreault, *Nano Lett.* **2010**, *10*, 2303.

[8] S. Nishimura, N. Abrams, B. A. Lewis, L. I. Halaoui, T.E. Mallouk, K. D. Benkstein, J. van de Lagemaat, A. Frank, *J. Am. Chem. Soc.* **2003**, *125*, 6306.

[9] L. I. Halaoui, N. M. Abrams, T. E. Mallouk, *J. Phys. Chem. B.* **2005**, *109*, 6334.

[10] A. Mihi, M. E. Calvo, J. A. Anta, H. Míguez, *J. Phys. Chem. C.* **2007**, *112*, 13.

[11] S. Colodrero, A. Mihi, L. Haggman, M. Ocana, G. Boschloo, A. Hagfeldt, H. Miguez, *Adv. Mater*. **2009**, *21*, 764.

[12] C. H. Yip, Y. M. Chiang, C. C. Wong, *J. Phys. Chem. C.* **2008,** *112*, 8735.

[13] J. I. L. Chen, G. Von Freymann, V. Kitaev, and G. A. Ozin, *J. Am. Chem. Soc.* **2007**, *129*, 1196.

[14] S. Colodrero, A. Mihi, J. A. Anta, M. Ocana, H. Míguez, *J. Phys. Chem. C.* **2009**, *113*, 1150.

[15] K. Sakoda, *Opt. Express*. **1999**, *4*, 167.

[16] D. M. Mittleman, J. F. Bertone, P. Jiang, K. S. Hwang, V. L. Colvin, *J. Chem. Phys.* **1999**, *111*, 345.

[17] P. Bermel, C. Luo, L. Zeng, L. C. Kimerling, J. D. Joannopoulos, *Opt. Express.* **2007**, *15*, 16986.

[18] P. G. O'Brien, N. P. Kherani, A. Chutinan, G. A. Ozin, S. John, S. Zukotynski, *Adv. Mater*. **2008**, *20*, 1577.

[19] S. Colodrero, M. Ocaña, H. Míguez, *Langmuir*. **2008**, *24*, 4430.

[20] K. A. Arpin, A. Mihi, H. T. Johnson, A. J. Baca, J. A. Rogers, J. A. Lewis, P.V. Braun, *Adv. Mater*. **2010**, *22* ,1084.

[21] S-H. A. Lee, N. M. Abrams, P. G. Hoertz, G. D. Barber, L. I. Halaoui, T. E. Mallouk, *J. Phys. Chem. B.* **2008**, *112*, 14415.

[22] K. Zhu, N. R. Neale, A. Miedaner, A. Frank, *Nano Lett.* **2006**, *7*, 69.

[23] D. Kim, A. Ghicov, S. P. Albu, P. Schmuki, *J. Am. Chem. Soc.* **2008**, *130*, 16454.

[24] J. M. Macak, H. Tsuchiya, P. Schmuki, *Angew. Chem. Int. Ed.* **2005**, *44*, 2100.

[25] G. Zhang, H. Huang, Y. Liu, L. Zhou, *Appl. Catal. B.* **2009**, *90*, 262.

[26] G. Zhang, H. Huang, Y. Zhang, H. L. W. Chan, L. Zhou, *Electrochem. Commun.* **2007**, *9*, 2854.

[27] J. Lin, K. Liu, X. Chen, *Small* **2011**, *7*, 1784.

[28] A. Mihi, H. Míguez, *Phys. Rev. B* **2005**, *71*, 125131-1.

[29] F. G.-Santamaría, E. C. Nelson, P. V. Braun, *Phys. Rev. B* **2007**, *76*, 075132-1.

[30] A. Mihi, F. J. Lopez-Alcaraz, H. Míguez, *Appl. Phys. Lett.* **2006**, *88*, 193110-1.

[31] B. Lee, D. K. Hwang, P. J. Guo, S. T. Ho, D. B. Buchholtz, C. Y. Wang, R. P. H. Chang, *J. Phys. Chem. B.* **2010**, *114*, 14582.

[32] C. A.Tao, W. Zhu, Q. An, G. T. Li, *J. Phys. Chem. C.* **2010**, *114*, 10641.

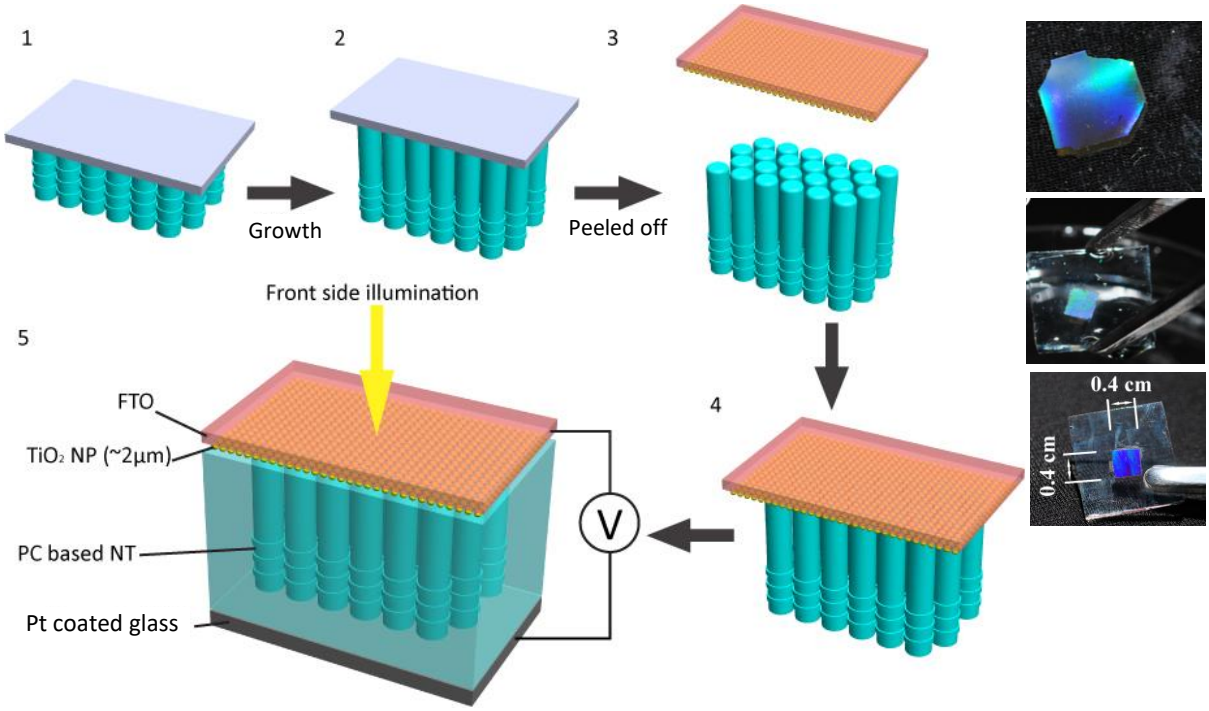

Figure 1. Schematic of the cell fabrication process. (1) Formation of PC layer. (2) Further formation of NT layer. (3) The bi-layer was detached from the Ti substrate. (4) The detached bi-layer was glued to a FTO substrate through TiO_2 nanoparticles. (5) Final assembly of the DSSC. The insets from the top to the bottom show the photographs of a typical sample in steps 3-5, respectively.

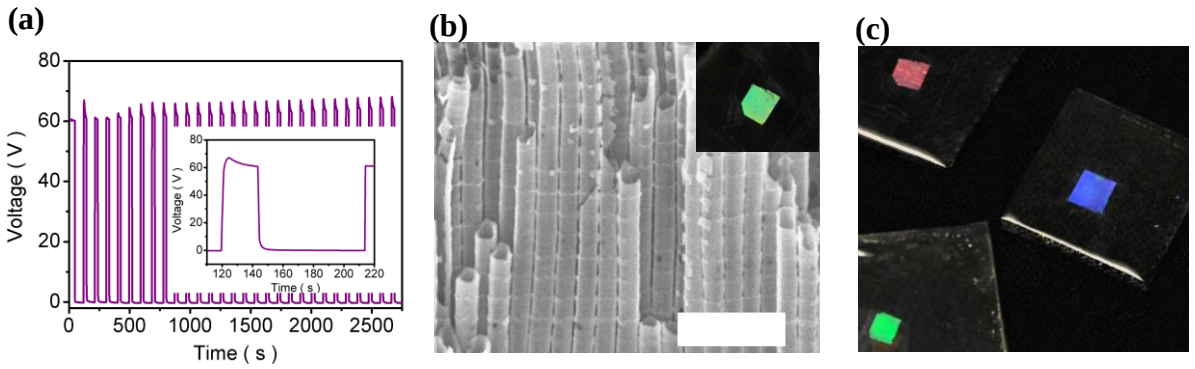

Figure 2. (a) Typical voltage–time (*V*-*t*) transient to fabricate the PC layer. Alternating LC (t_{LC}=180 s) and HC (t_{HC}=24 s) pulses were applied during the anodization. Inset: an enlarged *V*-*t* curve during 118-150 s. (b) Cross-section image of the fabricated PC layer. The scale bar measures 1 μm. Inset: the PC layer transferred onto FTO substrate showing a green color. (c) Photographs of PC samples (in ethanol) of various colors. The axial lattice constant of the PC layer can be tuned by the HC pulse duration t_{HC} to obtain PC layers of different colors. Longer wavelengths correspond to larger lattice constants (longer t_{HC}).

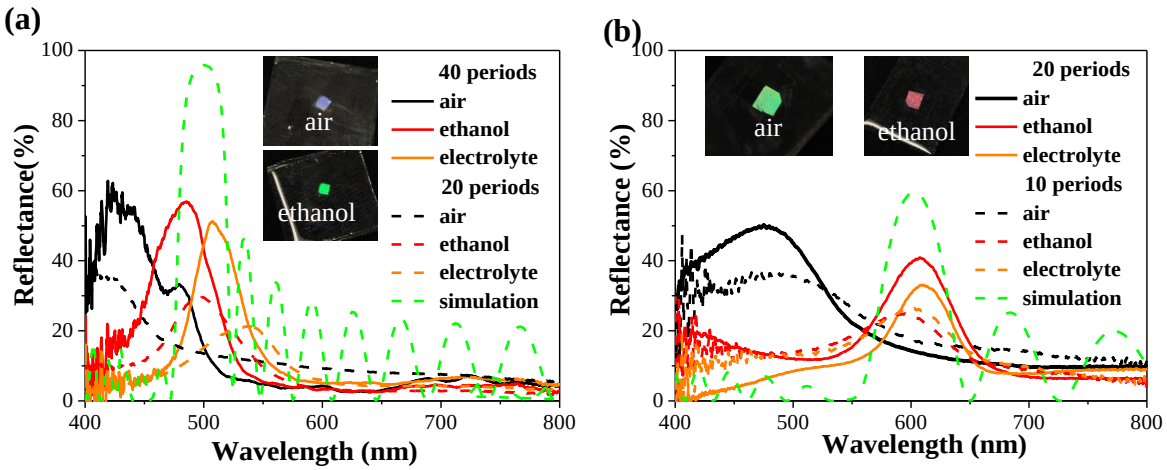

Figure 3 Reflectance spectra under near normal incidence of unpolarized light. (a) Reflectance on samples with 20 and 40 periods (lattice constant ~150 nm). (b) Reflectance on samples with 10 and 20 periods (lattice constant ~190 nm). The background reflectance from the FTO-coated glass substrate was subtracted. The insets show photographs of the samples (with 20 periods) in air and infiltrated with ethanol, respectively. The green curves are simulated results with lattice constant 150 and 190 nm for purple and green samples.

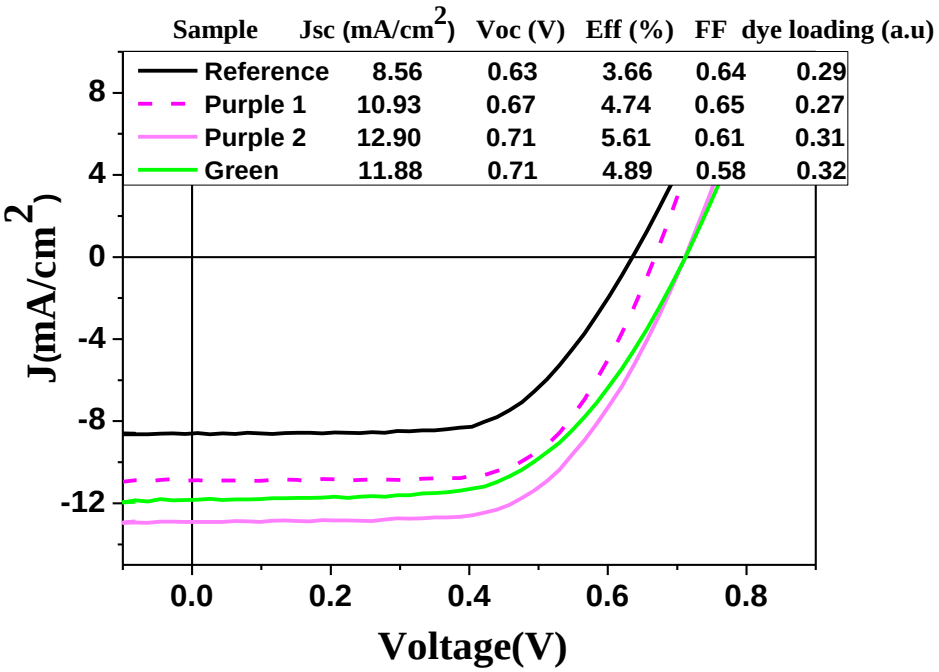

Figure 4 Photocurrent-voltage curves under AM 1.5 solar light illumination. Four cells, namely purple1, purple 2, green, and reference were tested. The axial lattice parameters in the PC layer of purple and green cells are ~150 and ~190 nm, respectively. The numbers of periods for the PC layer of the purple and green cells are 30 and 20, respectively, and the corresponding HC pulse durations (t_{HC}) are 28 and 40 s, respectively. Purple 1 and purple 2 are similar cells with slight difference in dye loading. The reference cell is similar to the others except for the exclusion of the PC layer.

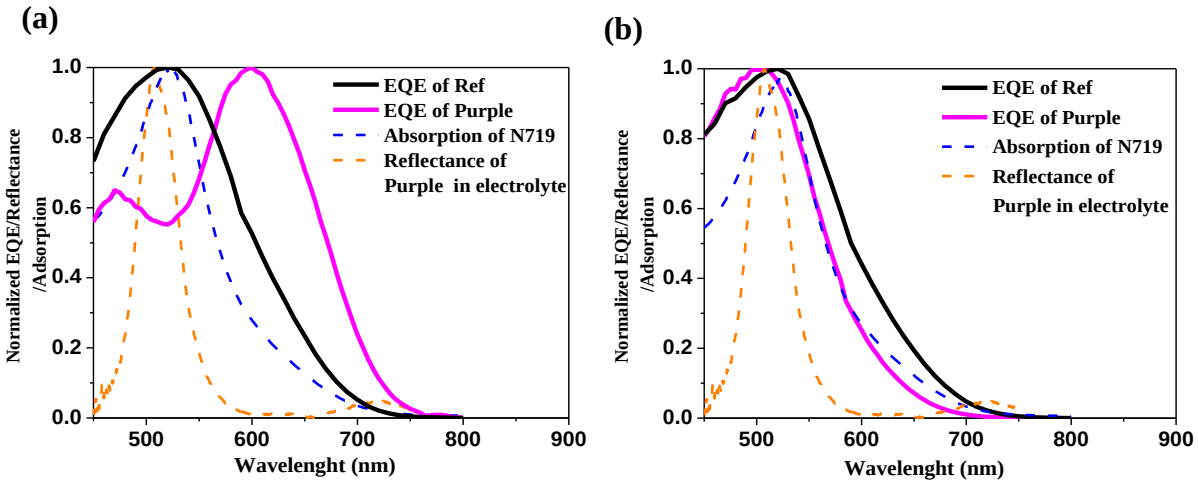

Figure 5 Normalized EQE of DSSCs with and without PC layer. A purple cell and a reference (Ref) one are compared. The reference cell is similar to the purple one but without the PC layer. Both cells have similar dye loading. (a) Back side illumination. (b) Front side illumination. The reflectance of the PC layer and the absorption of N719 are also shown in the figures for comparison.

Submitted to ADVANCED MATERIALS

Supporting Information

Direct and Seamless Coupling of TiO_2 Nanotube Photonic Crystal to Dye-Sensitized Solar Cell: A Single-Step Approach

By *Cho Tung Yip,[+] Haitao Huang,[+,] * Limin Zhou,* Keyu Xie, Yu Wang, Tianhua Feng, Jensen Li, and Wing Yim Tam*

Dr. C. T. Yip, Prof. L. Zhou
Department of Mechanical Engineering
The Hong Kong Polytechnic University
Hung Hom, Kowloon, Hong Kong
E-mail: mmlmzhou@inet.polyu.edu.hk

Prof. H. Huang, K. Xie, Prof. Y. Wang
Department of Applied Physics and Materials Research Center
The Hong Kong Polytechnic University
Hung Hom, Kowloon, Hong Kong,
E-mail: aphhuang@polyu.edu.hk

T. Feng, Prof. J. Li,
Department of Physics and Materials Science
City University of Hong Kong
Tat Chee Avenue, Kowloon, Hong Kong

Prof. W. Y. Tam
Department of Physics
Hong Kong University of Science and Technology
Clear Water Bay, Kowloon, Hong Kong

[+] C. T. Y. and H. H. contributed equally to this work.

Keywords: photonic crystal, dye-sensitized solar cell, TiO_2 nanotubes, electrochemical anodization

Microstructure

Figure S1 shows the cross-section image of a typical bi-layer structure on a titanium substrate. The PC layer can be found to seamlessly grown on top of the TiO_2 NT layer, which allows efficient infiltration of electrolyte.

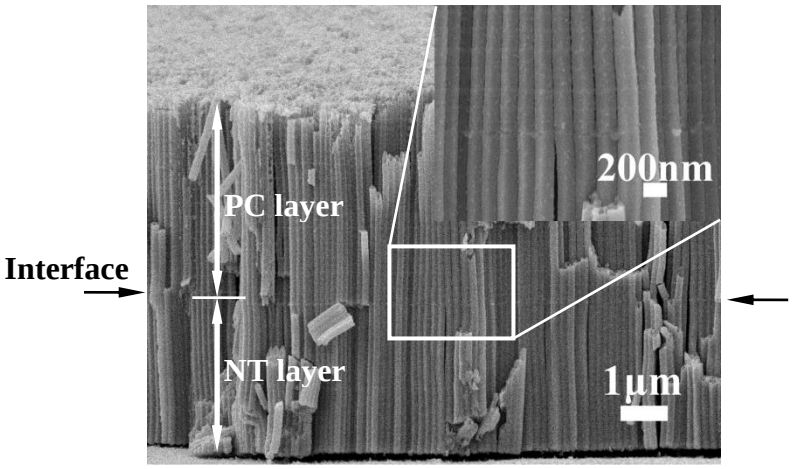

Figure S1. Cross-section of bi-layer structure. Inset: an enlarged part of the interface between the two layers.

Figure S2 shows the cross-section image of a typical bi-layer attached to the FTO substrate. The total length of the bi-layer structure is ~10 μm. The thickness of the mesoporous TiO_2 nanoparticle layer is around 2 μm.

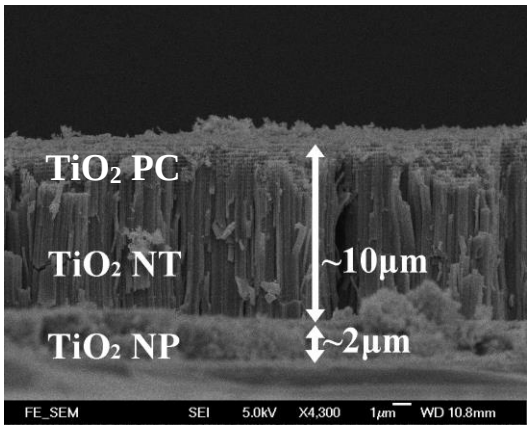

Figure S2. Cross-section image of a bi-layer attached to FTO substrate.

Figure S3 shows the cross-section image of the reference TiO_2 NT layer (without

periodicity along the tube direction) attached to FTO substrate. The length of TiO_2 NT is about 10 μm.

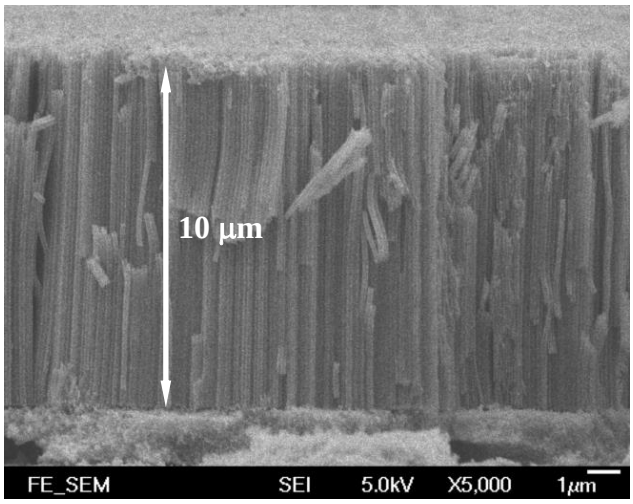

Figure S3. Cross-section image of a reference electrode attached to FTO substrate.

The top-view images of the bi-layer structure and a reference sample are shown in Fig.S4.

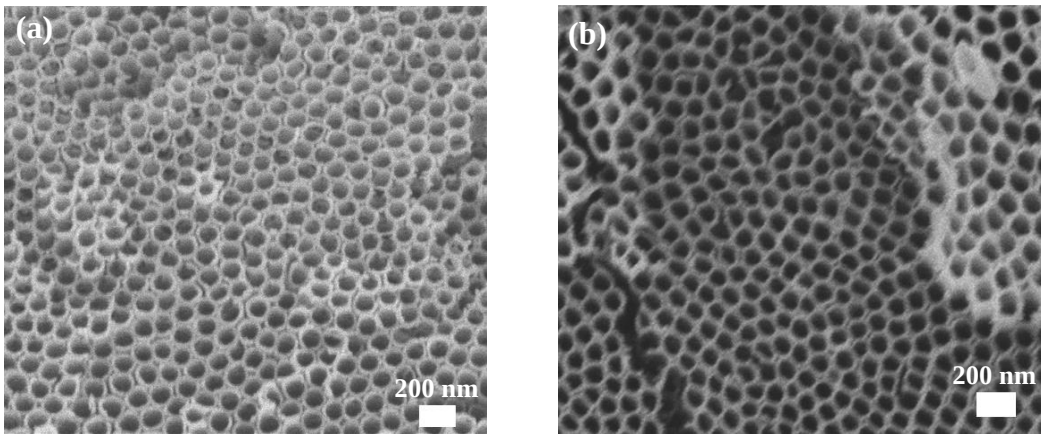

Figure S4 Top-view of the (a) bi-layer structure and (b) the reference sample.

Computation of Reflectance Spectra

Figure S5 shows the computer simulations on the reflectance spectra of two PC samples which are green and purple in ethanol. The axial lattice constants of the green and

purple samples are 190 and 150 nm, respectively. The peak reflectance of the purple sample locates at 500 nm and that of the green sample at 600 nm, both in agreement with experimental observations. The peak reflectance also increases in value with increasing number of periods.

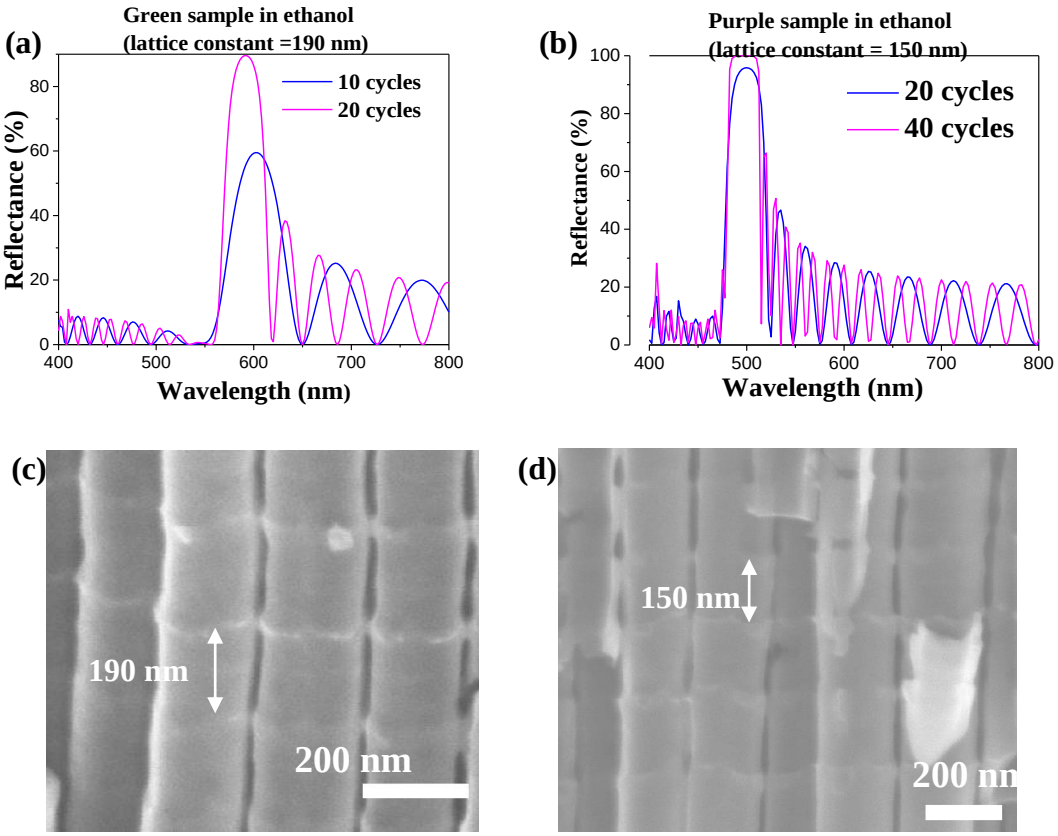

Figure S5. Computer simulations of the reflectance spectra and the corresponding microstructure. (a) Green sample in ethanol. (b) Purple sample in ethanol. (c) Cross-section image of green sample. (d) Cross-section image of purple sample.

EQE

Figure S6 shows the EQE spectra of a purple sample (the one in **Figure 5**) without normalization. It can be seen clearly that under back side illumination, the EQE is greatly reduced due to the blocking of light waves in the photonic bandgap and the strong absorption of light by the electrolyte. However, an EQE peak in a longer wavelength near the photonic

bandgap edge (600 nm) can be ascribed to the localization of red light in the TiO_2 of the PC layer. Under front side illumination, significant increase in EQE can be observed in a much wider spectrum range, indicating the enhanced light absorption by the coupling of the PC layer. It should be noted that our EQE results were obtained in the absence of bias light. Since EQE is light intensity dependent,[S1] it is incorrect to deduce the photocurrent from our EQE results. The photocurrent should be determined by the I-V measurement. The results shown here are only for comparative study of the PC effect.

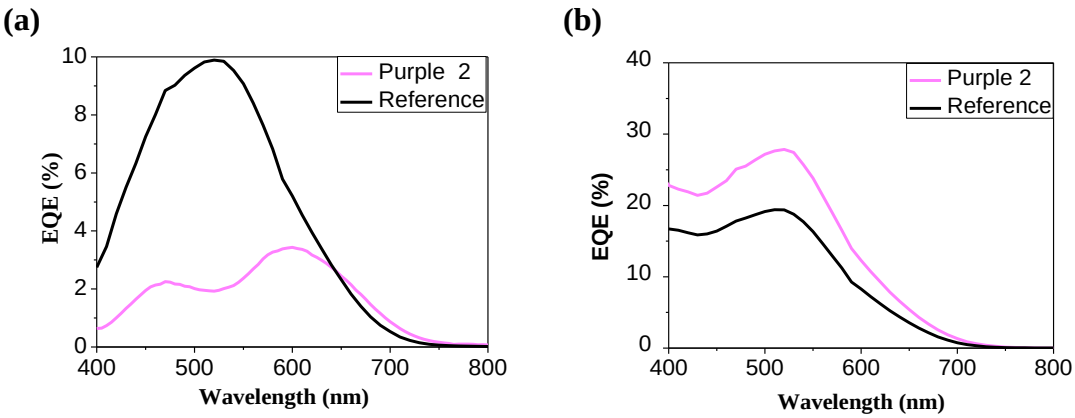

Figure S6. EQE spectra for purple sample without normalization. (a) Back side illumination. (b) Front side illumination.

Mechanism:

Figure S7 schematically illustrates the mechanism of enhanced light absorption due to the coupling of a PC layer to the TiO_2 absorption layer. Within the photonic bandgap, photons are reflected back to the absorption layer for further light harvesting. Additional resonance modes may also be formed within the absorption layer. At the longer wavelength edge of the photonic bandgap, the group velocity of light decreases anomalously to zero, which results in the photon localization in higher refractive index material (TiO_2, which is also attached to dye molecules) in the PC layer.[S2] This also increases the light harvesting.

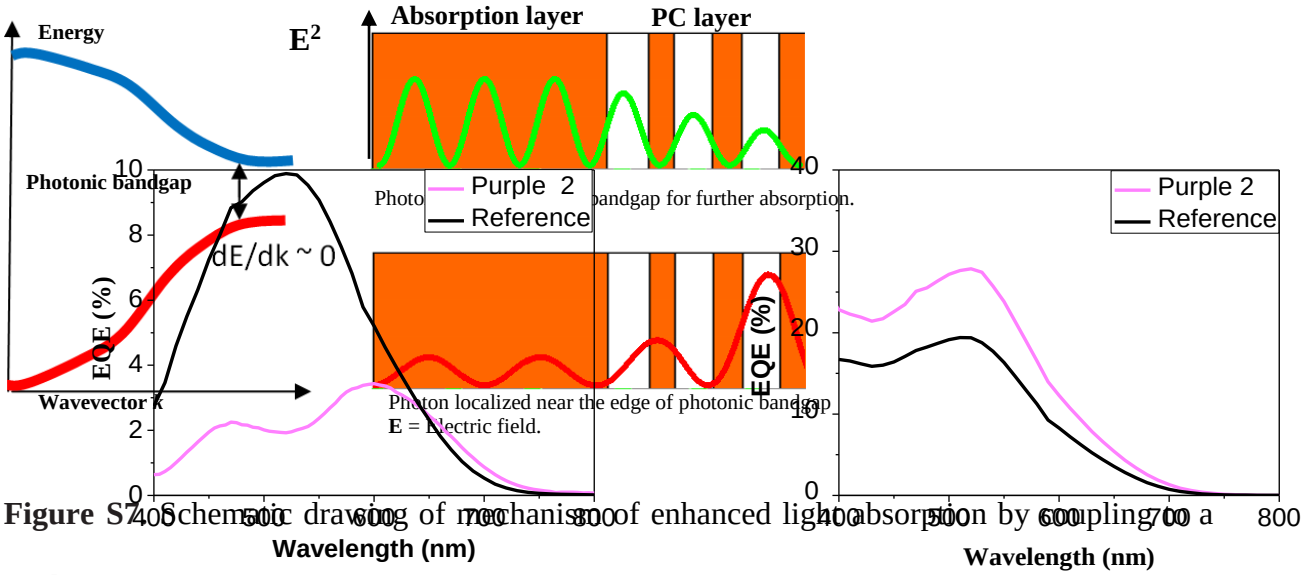

Figure S7. Schematic drawing of mechanism of enhanced light absorption by coupling to a PC layer.

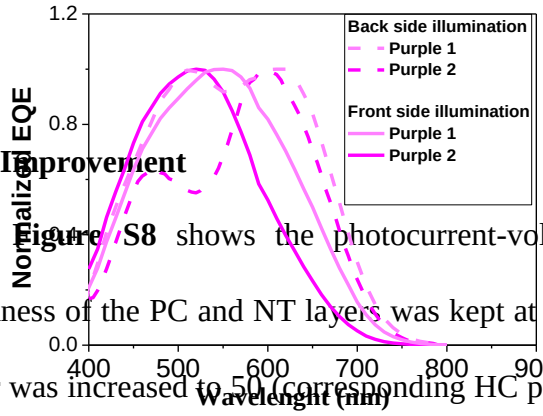

Cell Improvement

Figure S8 shows the photocurrent-voltage curve of an improved cell. The total thickness of the PC and NT layers was kept at 10 μm, while the number of periods of the PC layer was increased to 50 (corresponding HC pulse durations t_{HC}=28s). The power conversion efficiency and short circuit current were increased to 7.11% and 15.27 mA cm^{-2}, respectively, as compared with those of the purple 2 sample (**Figure 4**). The open circuit voltage and the fill factor remained similar to those of the purple 2 sample.

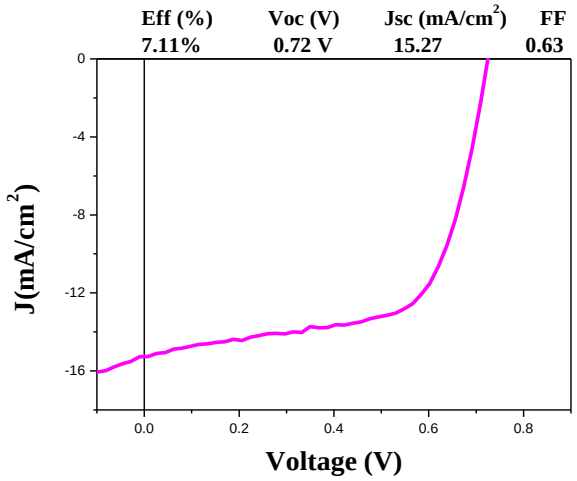

Figure S8. Photocurrent-voltage curves under AM 1.5 solar light illumination.

Mechanical Strength

A scotch tape method was used to test the adhesion of the PC layer to the photoanode. As shown in **Figure S9** (a), when the scotch tape was peeled off, part of the ink was transferred from a "T" (written by a maker before the test) on the glass substrate to the scotch tape. However, the PC layer was still attached to the photoanode, showing a good mechanical strength. The photo of a sealed solar cell is shown in **Figure S9** (b).

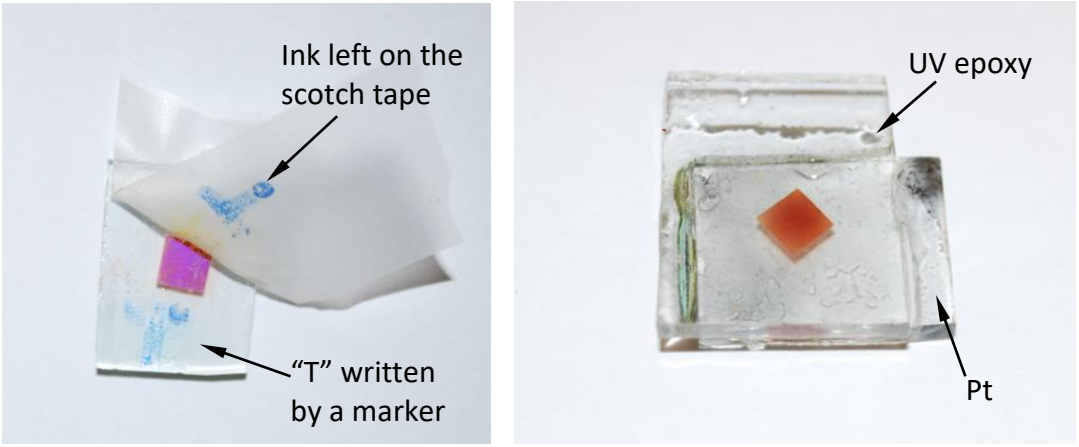

Figure S9 Photos of (a) a scotch tape test and (b) a sealed solar cell.

References

[S1] J. Y. Kim, J. H. Noh, K. Zhu, A. F. Halverson, N. R. Neale, S. Park, K. S. Hong, A. J. Frank, *ACS. Nano.***2011**, *5*, 2647.

[S2] S. Nishimura, N. Abrams, B. A. Lewis, L. I. Halaoui, T. E. Mallouk, K. D. Benkstein, J. van de Lagemaat, A. J. Frank, *J. Am. Chem. Soc.* **2003**, *125*, 6306.

Table of Contents:

A TiO_2 nanotube layer with a periodic structure was used as a photonic crystal to greatly enhance light harvesting in TiO_2 nanotube based DSSCs. Such a tube-on-tube structure fabricated by a single-step approach facilitates good physical contact, easy electrolyte infiltration and efficient charge transport. An increase of over 50% in power conversion efficiency was obtained when compared with reference cells without a photonic crystal layer (under similar total thickness and dye loading).